

See discussions, stats, and author profiles for this publication at: <https://www.researchgate.net/publication/41434045>

# Thermal Decomposition of a Melt-Castable High Explosive: Isoconversional Analysis of TNAZ

ARTICLE *in* THE JOURNAL OF PHYSICAL CHEMISTRY B · MARCH 2002

Impact Factor: 3.3 · DOI: 10.1021/jp012859o · Source: OAI

---

CITATIONS

9

---

READS

23

2 AUTHORS, INCLUDING:



[Charles A. Wight](#)

Weber State University

141 PUBLICATIONS 3,633 CITATIONS

SEE PROFILE

# Thermal Decomposition of a Melt-Castable High Explosive: Isoconversional Analysis of TNAZ

Gregory T. Long and Charles A. Wight\*

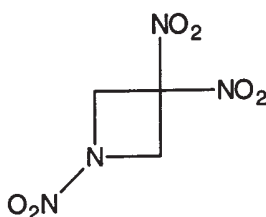
Center for Thermal Analysis, Department of Chemistry, University of Utah, Salt Lake City, Utah 84112

Received: July 24, 2001; In Final Form: December 6, 2001

The thermal decomposition kinetics of the high explosive 1,3,3-trinitroazetidine (TNAZ) have been measured by nonisothermal differential scanning calorimetry (DSC). Samples of TNAZ in open pans and pierced pans undergo mainly melting ( $\Delta H_{\text{fus}} = 27 \pm 3 \text{ kJ mol}^{-1}$ ) and vaporization ( $\Delta H_{\text{vap}} = 74 \pm 10 \text{ kJ mol}^{-1}$ ) during heating. However, when confined in sealed high-pressure crucibles, exothermic thermal decomposition is observed. The activation energy for thermal decomposition has been determined as a function of the extent of reaction by isoconversional analysis. The initial value of  $184 \text{ kJ mol}^{-1}$  at the start of the reaction decreases to  $38 \text{ kJ mol}^{-1}$  near the end of the reaction. The rates clearly exhibit acceleratory behavior that is ascribed to autocatalysis. The measured heat release of thermal decomposition ( $Q = 640 \pm 150 \text{ kJ mol}^{-1}$ ) is independent of the heating rate and the sample mass. These results are consistent with proposed mechanisms of TNAZ decomposition in which the initial step is preferential loss of the nitramine  $\text{NO}_2$  group over loss of a *gem*-dinitroalkyl  $\text{NO}_2$  group.

## Introduction

The four membered *gem*-dinitroalkyl cyclic nitramine, 1,3,3-trinitroazetidine



(TNAZ) has very desirable properties of an explosive. It has a melting point ( $101^\circ\text{C}$ ) that is considerably below the limit of its thermal stability ( $<240^\circ\text{C}$ ),<sup>1</sup> and this allows TNAZ to be melt-cast.<sup>2</sup> Currently, trinitrotoluene (TNT) is the only widely used melt-castable explosive, and TNAZ therefore is being considered as an alternative or replacement for TNT in this application.<sup>2,3</sup> Moreover, TNAZ has been shown to be more powerful and less sensitive than the most powerful military explosive formulation.<sup>2</sup> The more desirable characteristics of TNAZ compared to the larger six- and eight-membered cyclic nitramines, hexahydro-1,3,5-trinitro-1,3,5-triazine (RDX) and octahydro-1,3,5,7-tetranitro-1,3,5,7-tetrazocine (HMX), has led to the consideration of the use of TNAZ in both explosive<sup>2</sup> and propellant<sup>4</sup> applications.

An important aspect of characterizing an explosive is the determination of the kinetics and associated energetics of its thermal decomposition. To the best of our knowledge, there have been two reports of the Arrhenius parameters for the decomposition of TNAZ.<sup>5,6</sup> Both were thermolysis studies and were conducted isothermally in sealed capillaries and analyzed by GC-MS. Kinetic measurements over a temperature range of

$220\text{--}250^\circ\text{C}$  gave Arrhenius values of  $E_A = 183 \text{ kJ mol}^{-1}$  and  $A = 1.85 \times 10^{16} \text{ s}^{-1}$ <sup>5</sup> and those over a range of  $160\text{--}250^\circ\text{C}$  yielded values of  $E_A = 195 \text{ kJ mol}^{-1}$  and  $A = 3.55 \times 10^{17} \text{ s}^{-1}$ .<sup>6</sup>

It is now known that the assignment of a single value of activation energy to a thermal decomposition process can be an incomplete and inadequate description of the kinetics. The decomposition reactions of several explosives, including TNAZ<sup>7</sup> and NTO,<sup>8</sup> have been reported to be autocatalytic; we can therefore expect that the activation energy for the overall (global) reaction should decrease as the reaction proceeds through the autocatalytic phase.<sup>9</sup> More generally, solid-state processes are most often comprised of multiple competing processes, both physical (polymorphic transition, diffusion, sublimation, adsorption, desorption) and chemical (solid-state decomposition, product reactions with the solid, and gas-phase reactions) in character.<sup>10</sup> The kinetic competition of these processes usually leads to global activation energies that change during the course of the reaction. Hence, it is desirable to analyze the kinetics of these reactions in a way that allows the activation energy ( $E_\alpha$ ) and preexponential factor ( $A$ ) to vary with the extent of reaction,  $\alpha$ , to provide a more complete and accurate description of the kinetics.

Our approach to this problem has been to employ a model-free isoconversional analysis of thermal analysis experiments such as DSC and thermogravimetric analysis (TGA).<sup>11–13</sup> This methodology has been applied successfully to NTO<sup>9</sup> and the cyclic nitramines, HMX<sup>14</sup> and RDX.<sup>15</sup> Conceptually, the strategy is to carry out several experiments using different heating rates to set up a competition between the rate of heating and the rate of reaction. The experiments are compared with each other at the same extent of reaction (e.g., 10% decomposition) to extract an activation energy and preexponential factor on the basis of the differences in thermal histories of the experiments up to that point (hence the term, *isoconversional*). By repeating the

\* Corresponding author. E-mail: wight@chem.utah.edu.

analysis at many different extents of reaction, it is possible to numerically evaluate the dependence of  $E_A$  and  $A$  on the extent of reaction without the need to assume any particular form of the reaction model (e.g., first-order, second-order, etc.) prior to the analysis (hence the term, *model-free*). In practice, it is possible to carry out experiments that are not restricted to constant-rate heating programs, and we can perform the analysis for sets of experiments using isothermal, linear, and arbitrary heating programs. The most reliable results are usually obtained by analyzing sets of experiments that utilize the widest practical variation in temperature programs.

Using nonisothermal DSC, Bulusu and co-workers observed that TNAZ melts at  $\sim 95^\circ\text{C}$ . In pierced pans, subsequent vaporization of the liquid TNAZ leads to escape of the material through the opening in the sample pan. However, in closed pans both melting and decomposition ( $200\text{--}240^\circ\text{C}$ ) are observed.<sup>16</sup> In this paper we report the kinetics of thermal decomposition of TNAZ using isoconversional analysis of nonisothermal DSC experiments in closed pans. The activation energy is observed to decrease with the extent of reaction,  $\alpha$ , providing strong support for the role of autocatalysis in the mechanism. The initial magnitude of  $E_\alpha$  is consistent with decomposition mechanisms that invoke preferential N–NO<sub>2</sub> bond scission over C–NO<sub>2</sub> bond scission as the initial step.<sup>6,7,17,18</sup> Our work therefore provides a more complete understanding of the thermal stability of TNAZ that can be used to optimize safety and cost-effectiveness in its manufacture, handling, and storage.

## Experimental Section

TNAZ, obtained from Lawrence Livermore National Laboratory, was used as received and studied as a granular powder.

DSC traces collected for nonisothermal heating programs employed a Mettler-Toledo DSC821<sup>e</sup> module. Open and pierced pan experiments used 40  $\mu\text{L}$  Al pans and closed pan experiments used 30  $\mu\text{L}$  stainless steel high-pressure crucibles. N<sub>2</sub> gas flowing at a rate of 80 mL min<sup>-1</sup> served as the purge gas. For a heating rate of  $\beta = 10.0^\circ\text{C min}^{-1}$ , sample sizes of 1.0 and 0.5 mg were used in nonisothermal open and pierced pan experiments, respectively. Pans lidded with crimp-sealed Al piercing lids were punctured with a 1.0 mm piercer immediately prior to insertion in the calorimeter. DSC traces were collected for  $\sim 0.2$  mg TNAZ samples sealed in high-pressure crucibles. Nonisothermal closed-pan DSC experiments employed heating rates of  $\beta = 2.5, 5.0, 7.5, 10.0, 12.5, 15.0, 17.5,$  and  $20.0^\circ\text{C min}^{-1}$ .

All of the uncertainties given in this paper represent 95% confidence limits for the indicated quantity. In most cases, the uncertainties arise from statistical uncertainties in measured quantities. However, uncertainties in the activation energies also include systematic errors arising from errors in assumptions of the kinetic equations.

**Kinetic Analysis.** The decomposition kinetics of a heterogeneous solid-state reaction are typically described by the equation<sup>19</sup>

$$\frac{d\alpha}{dt} = k(T)f(\alpha) = Ae^{-E/RT}f(\alpha) \quad (1)$$

where  $\alpha$  is the extent of reaction and  $f(\alpha)$  is the reaction model, which gives the dependence of the reaction rate on the extent of reaction. For gas-phase reactions, the reaction model usually takes a simple first-order or second-order form. In the second part of eq 1, the Arrhenius equation has been substituted for the temperature-dependent rate constant,  $k(T)$ . Rearranging this

equation by separating  $\alpha$  and  $t$  and integrating, leads to an equation that describes the integrated reaction model,  $g(\alpha)$ :

$$\int_0^\alpha \frac{d\alpha}{f(\alpha)} = g(\alpha) = A \int_0^{t_\alpha} e^{-E/RT(t)} dt = AJ[E, T(t_\alpha)] \quad (2)$$

where  $\alpha$  describes the values pertaining to a particular extent of conversion. Model-free isoconversional methods use  $g(\alpha)$  to determine activation energies from thermal analysis data as a function of  $\alpha$ .<sup>12,13</sup> This approach assumes that the reaction model is independent of the temperature program. From this assumption, the right hand sides of eq 2 are all equal for experiments conducted under different heating programs. To solve this equation for  $n$  such experiments,  $E_\alpha$  can be determined for any chosen  $\alpha$  by solving for the activation energy that minimizes the function

$$S^2(E_\alpha) = \frac{1}{n(n-1)} \sum_{i=1}^n \sum_{j \neq i}^n \left( \frac{J[E_\alpha, T_i(t_\alpha)]}{J[E_\alpha, T_j(t_\alpha)]} - 1 \right)^2 \quad (3)$$

where the subscripts  $i$  and  $j$  denote indices for two experiments performed under different heating programs. The integral,  $J$ , in this equation is solved numerically with the trapezoid rule. To account for the variation of activation energy with the extent of conversion, the experimental kinetic traces are broken up into segments (e.g., each 5% of the extent of reaction is analyzed independent of the other segments).<sup>13</sup>  $E_\alpha$  for each segment is calculated by numerical integration of the  $T(t)$  data over that segment:

$$J[E_\alpha, T_i(t_\alpha)] \equiv \int_{t_{\alpha-\Delta\alpha}}^{t_\alpha} e^{-E_\alpha/RT(t)} dt \quad (4)$$

Typically, the extent of reaction is broken down into 10–50 different segments, and the analysis is repeated for each segment in order to obtain the activation energy as a function of the extent of reaction.

For a complete description of the kinetics (e.g., to make kinetic rate predictions), it is also necessary to extract the values of  $A$  and  $f(\alpha)$  from the data. If the number of reaction segments is sufficiently large that  $f(\alpha)$  can be considered to be constant,  $f$ , within a given segment, then separation of variables in eq 1 gives

$$\frac{1}{Af} \int_{\alpha-\Delta\alpha}^\alpha d\alpha' = \int_{t_{\alpha-\Delta\alpha}}^{t_\alpha} e^{-E/RT(t)} dt \quad (5)$$

and integration over the segment and rearrangement yields

$$Af = \frac{\Delta\alpha}{J[E_\alpha, T_i(t_\alpha)]} \quad (6)$$

where  $J$  is the Arrhenius integral for the given segment from eq 4. Thus, for a given segment, it is straightforward to determine the product  $Af$ . Repeating this procedure for each segment builds up the  $\alpha$ -dependence over the entire reaction,  $Af(\alpha)$ . Because the separation of the constant  $A$  and the function  $f(\alpha)$  is arbitrary, we represent this combined quantity as  $A(\alpha)$ .

Confidence intervals for the activation energies have been estimated statistically.<sup>12</sup> The  $J$ -integrals (eq 4) for any given segment ( $t_{\alpha-\Delta\alpha} \rightarrow t_\alpha$ ) should be equal for all experiments under the assumption that the reaction model is independent of the temperature program,  $T(t)$  (cf., eq 2). Thus, the variance,  $S^2$ , in eq 3 should be independent of the number of experiments, apart from statistical fluctuations in the experimental data. The optimal value of the activation energy,  $E_{\min}$ , is determined by minimizing

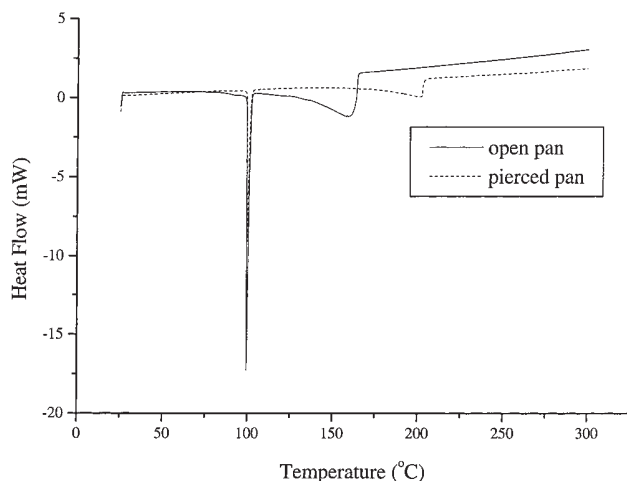


**Figure 1.** Open-pan and pierced-pan DSC traces of TNAZ both acquired at a constant heating rate of  $\beta = 10\text{ }^{\circ}\text{C min}^{-1}$ . The negative-going bands depict endothermic processes.

$S^2$ . For this case, the statistics

$$\Psi(E_{\alpha}) = \frac{S^2(E_{\alpha})}{S_{\min}^2} \quad (7)$$

have the  $F$ -distribution.<sup>20,21</sup> These statistics allow the confidence limits for  $E_{\min}$  to be determined from estimating the confidence limits for the variance,  $S_{\min}^2$ . For the condition

$$\Psi(E_{\alpha}) < F_{1-p, n-1, n-1} \quad (8)$$

where  $F_{1-p, n-1, n-1}$  is a percentile of the  $F$ -distribution for  $(1 - p) \times 100\%$  confidence probability, the  $p \times 100\%$  confidence interval for  $S_{\min}^2$  can be calculated. Then the upper and lower confidence limits ( $E_{\alpha}^{lo}$  and  $E_{\alpha}^{up}$ , respectively) for  $E_{\alpha}^{\min}$  can be estimated as the value of  $E_{\alpha}$  for which  $\Psi(E_{\alpha}) = F_{1-p, n-1, n-1}$ . Error limits given for  $E_{\alpha}$  in this paper were determined using  $p = 0.05$  and therefore represent 95% confidence intervals.

## Results

**Open Pan and Pierced Pan Samples.** DSC traces collected for open pan and pierced pan samples of TNAZ both show sharp endotherms at 99 °C (Figure 1). A broad endotherm that occurs between 105 and 165 °C in an open pan shifts to between 145 and 205 °C in the more confined environment of a pierced pan. Integration and normalization of the heat release of the endotherms leads to values of the heat of reaction of  $Q_1 = 27 \pm 3\text{ kJ mol}^{-1}$  for the sharp endotherm and  $Q_2 = 74 \pm 10\text{ kJ mol}^{-1}$  for the broad endotherm. The error limits represent 95% confidence intervals.

**Closed Pan Samples.** A nonisothermal DSC experiment on a closed pan sample of TNAZ at a heating rate of  $\beta = 10.0\text{ }^{\circ}\text{C min}^{-1}$  exhibits a sharp melting endotherm at 99 °C and a decomposition exotherm between 220 and 290 °C (Figure 2a). Isoconversional analysis of the exotherm yields a set of activation energies that decrease from  $E_{\alpha} = 184\text{ kJ mol}^{-1}$  at  $\alpha = 0.01$  to  $E_{\alpha} = 38\text{ kJ mol}^{-1}$  at  $\alpha = 0.99$  (Figure 2b). To further characterize TNAZ decomposition, the integrated and normalized heat release in DSC traces was monitored as a function of both heating rate and the mass. These experiments give a rather constant heat release of  $Q = 640 \pm 150\text{ kJ mol}^{-1}$  (95% confidence interval) that is independent of  $\beta$  and of the sample mass for closed pan samples (Figure 3).

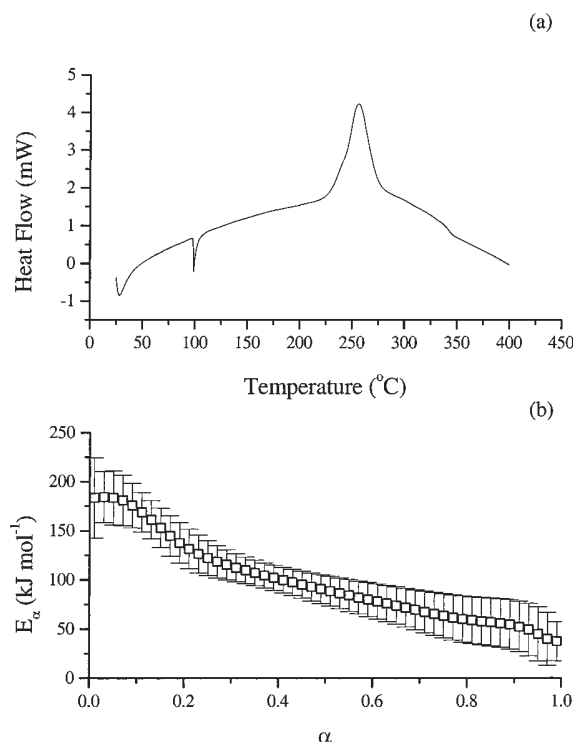


**Figure 2.** (a) A nonisothermal DSC trace acquired at a heating rate of  $\beta = 10\text{ }^{\circ}\text{C min}^{-1}$  for a closed pan sample of TNAZ. The positive-going band near 250 °C is attributed to exothermic thermal decomposition. (b) A plot of  $E_{\alpha}$  as a function of  $\alpha$  created by isoconversional kinetic analysis of the exotherms from eight different experiments conducted at heating rates  $\beta = 2.5, 5.0, 7.5, 10.0, 12.5, 15.0, 17.5,$  and  $20.0\text{ }^{\circ}\text{C min}^{-1}$ .

In addition to the activation energies, the kinetic analysis also yields the Arrhenius preexponential factor. Referring to eq 6, it is possible to extract the value of the product  $Af$  for each segment of the reaction. For simplicity, we call this  $A(\alpha)$  because it not only provides the scaling factor required to compute the correct reaction rate within each segment, it also provides the dependence of the rate on the extent of reaction (i.e., the numerically evaluated reaction model). Figure 4 shows that for TNAZ decomposition the reaction model decreases with the extent of reaction in a manner that is approximately exponential in character (i.e., linearly decreasing value of  $\log[A(\alpha)]$  vs  $\alpha$ ).

## Discussion

**Open and Pierced Pan Samples.** The sharp endotherm that peaks at 99 °C in both open and pierced pan DSC traces has been previously assigned to melting (Figure 1).<sup>16</sup> The broad endotherm between 105 and 165 °C for open pan samples is indicative of vaporization.<sup>22</sup> This broad endotherm shifts to 145–205 °C in the semi-confined environment of a pierced pan sample and indicates some kinetic suppression of vaporization in the more confined sample environment. Because these experiments were carried out at constant pressure, the enthalpies for melting and vaporization are determined to be  $\Delta H_{\text{fus}} = 27 \pm 3\text{ kJ mol}^{-1}$  and  $\Delta H_{\text{vap}} = 74 \pm 10\text{ kJ mol}^{-1}$  from the respective endotherms. To our knowledge, this is the first published report of these values.

**Closed Pan Samples.** The functional dependence of  $E_{\alpha}$  on  $\alpha$  determined by isoconversional kinetic analysis of nonisothermal (Figure 2) DSC traces exhibits a decrease from an initial value ( $\alpha = 0.01$ ) of  $E_{\alpha} = 184\text{ kJ mol}^{-1}$ . This initial value is in good agreement with the two separate studies of the decomposi-

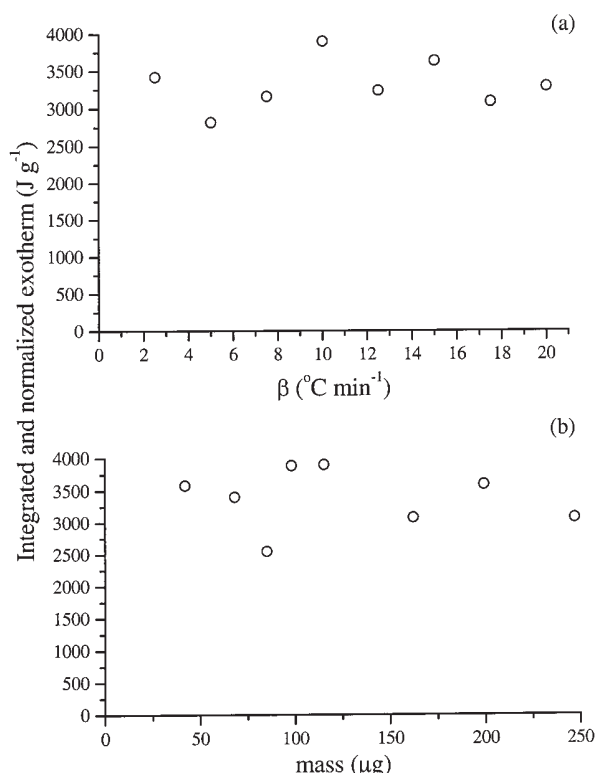


**Figure 3.** (a) Plot of the integrated and normalized exotherm as a function of  $\beta$  for  $\sim 120 \mu\text{g}$  closed pan samples of TNAZ. (b) A plot of the integrated and normalized exotherm in DSC traces of closed pan samples of TNAZ as a function of the mass at a heating rate of  $\beta = 10.0 \text{ }^\circ\text{C min}^{-1}$ .

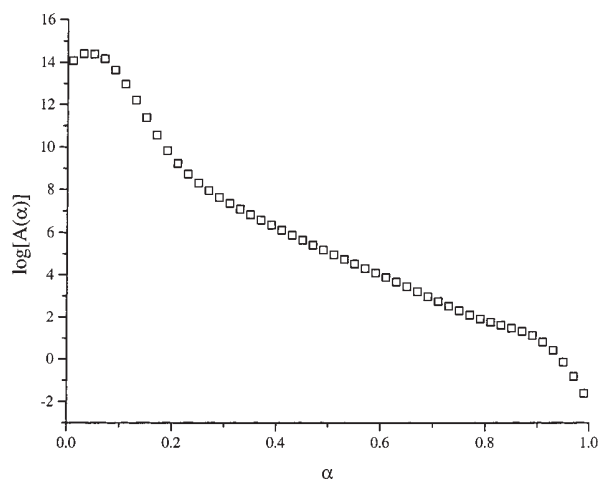


**Figure 4.** A plot of  $\log[A(\alpha)]$  versus  $\alpha$  for closed pan samples of TNAZ determined by isoconversional analysis of nonisothermal DSC traces.

tion kinetics and energetics of TNAZ by Oxley who reported activation energies of  $E_A = 183 \text{ kJ mol}^{-1}$ <sup>5</sup> and  $E_A = 195 \text{ kJ mol}^{-1}$ .<sup>6</sup>

The initial value of the activation energy determined in the current study is consistent with proposed decomposition mechanisms in the TNAZ literature. Many studies assert that several mechanisms occur, with  $\text{NO}_2$  loss being one of the first steps.<sup>6,7,17,18,23–27</sup> Further, there is experimental<sup>6,7,17,18</sup> and theoretical<sup>28</sup> evidence supporting  $\text{N–NO}_2$  loss to be favored over  $\text{C–NO}_2$  loss. For example, density functional theory (DFT) was used to calculate an  $\text{N–NO}_2$  bond dissociation energy (BDE) of  $187 \text{ kJ mol}^{-1}$  and a  $\text{C–NO}_2$  BDE of  $195 \text{ kJ mol}^{-1}$ .<sup>28</sup>

By way of comparison, our initial activation energy for TNAZ decomposition of  $E_a = 184 \text{ kJ mol}^{-1}$  also supports initial preferential  $\text{N–NO}_2$  scission. The observation of  $\text{NO}_2$  and  $\text{NO}$  as major initial products in the decomposition gases for TNAZ thermolysis for both high heating rate ( $50\text{--}170 \text{ }^\circ\text{C s}^{-1}$ )<sup>23</sup> and isothermal conditions<sup>7,17</sup> shows further consistency with the present work.

Experimental evidence suggests that autocatalysis plays a role during the thermal decomposition of TNAZ. For example, the activation energy decreases with  $\alpha$  for closed pan samples in nonisothermal DSC traces (Figure 2). The source of this catalysis may be a surface mechanism proposed by Behrens for both TNAZ and 1-nitroso-3,3-dinitroazetidine (NDNAZ), a minor product of TNAZ thermal decomposition.<sup>7</sup> Enhanced decomposition of both TNAZ and NDNAZ occurs when NDNAZ is added to a residue-coated cell and when clean microscopic ( $100 \mu\text{m}$ ) glass beads are added to the reaction cell.<sup>7</sup>

The determination of the dependencies of  $E_a$  and  $A(\alpha)$  using isoconversional analysis provides a comprehensive description of the decomposition kinetics of a heterogeneous solid-state reaction. For any particular extent of reaction  $\alpha$ , the reaction rate is predicted to be

$$\frac{d\alpha}{dt} = A(\alpha) e^{-E_a/RT} \quad (9)$$

where the values of  $E_a$  and  $A(\alpha)$  are given in Figures 2b and 4, respectively.

The heat of reaction  $Q = 640 \pm 150 \text{ kJ mol}^{-1}$  has been determined for the thermal decomposition of TNAZ under slow cook-off conditions. It is unlikely that the products formed in our experiments are the thermodynamically stable end products of TNAZ combustion. Rather, they are metastable intermediates formed in the initial decomposition reactions that transform liquid TNAZ into small gas-phase molecules. Therefore, our value of  $Q$  should not be compared with the heat of combustion, but may instead be associated with initial heat release at the burning surface (i.e., prior to heat release in the gas-phase flame).

## Conclusions

Our isoconversional kinetic analysis study of the thermal decomposition of TNAZ has determined decomposition kinetics and activation energies over the entire reaction. This information serves to unify several results in the TNAZ thermal decomposition literature. First, the initial activation energy  $E_a = 184 \text{ kJ mol}^{-1}$  from analysis of nonisothermal DSC traces is in good agreement with two previous reports of single values of activation energies.<sup>5,6</sup> Second, the activation energy is also in good agreement with a DFT calculation of an  $\text{N–NO}_2$  BDE of  $187 \text{ kJ mol}^{-1}$ <sup>28</sup> and with  $\text{N–N}$  bond scission being the preferential  $\text{NO}_2$  loss channel. Third,  $\text{NO}_2$  loss occurring as an initial decomposition step is in agreement with product analysis studies under both isothermal<sup>7,17</sup> and nonisothermal<sup>23</sup> conditions in which  $\text{NO}_2$  and  $\text{NO}$  are determined as major initial products of TNAZ thermal decomposition. Fourth, the observed decrease in  $E_a$  with  $\alpha$  is consistent with reports of autocatalysis during TNAZ decomposition. Such insight, which provides a more complete understanding of thermal decomposition and slow cook-off chemistry of TNAZ, may lead to the safer manufacture, handling, and storage of this explosive and similar energetic materials.

**Acknowledgment.** We thank Mettler-Toledo, Inc., for the generous donation of the DSC instrument used in this study.



We also thank Dr. Randy Simpson of Lawrence Livermore National Laboratory for providing the TNAZ sample. Partial support for this work from the Ballistic Missile Defense Organization and the Office of Naval Research under MURI Contract No. N00014-95-1-1339 and from the University of Utah Center for Simulation of Accidental Fires and Explosions is gratefully acknowledged.

## References and Notes

- (1) Piper, L. B.; Filliben, J. D. New High-Energy Oxidizers. CPIA Report, 93-52, Dec. 1993.
- (2) Iyer, S.; Eng, Y. S.; Joyce, M.; Perez, R.; Alster, J.; Stec, D. *Proceedings of the Joint International Symposium on Compatibility of Plastics and Other Materials with Explosives, Propellants, Pyrotechnics and Processing of Explosives, Propellants, and Ingredients*; San Diego, CA, April 1991; p 80.
- (3) Archibald, T. G.; Gilardi, R.; Baum, K.; George, C. *J. Org. Chem.* **1990**, *55*, 2920.
- (4) Oyumi, Y.; Brill, T. B.; Rheingold, A. L.; Haller, T. M. *J. Phys. Chem.* **1985**, *89*, 4317.
- (5) Oxley, J. C.; Kooh, A. B.; Szekeres, R.; Zhang, W. *J. Phys. Chem.* **1994**, *98*, 7004.
- (6) Oxley, J.; Smith, J.; Zheng, W.; Rogers, E.; Coburn, M. *J. Phys. Chem. A* **1997**, *101*, 4375.
- (7) Anderson, K.; Homsy, J.; Behrens, R.; Bulusu, S. *Sandia Combustion Research Technical Review*; 1998.
- (8) Bowden, F. P.; Yoffe, A. D. *Initiation and Growth of Explosion in Liquids and Solids*; Cambridge University Press: Cambridge, U. K., 1952 (reissued 1985); Chapter 1.
- (9) Long, G. T.; Brems, B. A.; Wight, C. A. *J. Phys. Chem. B*, submitted.
- (10) Vyazovkin, S.; Wight, C. A. *J. Phys. Chem. A* **1997**, *101*, 8279.
- (11) Vyazovkin, S.; Wight, C. A. *Annu. Rev. Phys. Chem.* **1997**, *48*, 125.
- (12) Vyazovkin, S.; Wight, C. A. *Anal. Chem.* **2000**, *72*, 3171.
- (13) Vyazovkin, S. *J. Comput. Chem.* **2001**, *22*, 178.
- (14) Lofy, P. M. S. Thesis, University of Utah, Salt Lake City, UT, 1999.
- (15) Long, G. T.; Vyazovkin, S.; Brems, B. A.; Wight, C. A. *J. Phys. Chem. B* **2000**, *104*, 2570.
- (16) Cahill, S.; Rinzler, A. G.; Owens, F. J.; Bulusu, S. *J. Phys. Chem.* **1994**, *98*, 7095.
- (17) Behrens, R.; Bulusu, S. *Def. Sci. J.* **1996**, *46*, 361.
- (18) Garland, N. L.; Nelson, H. H. *J. Phys. Chem. B* **1998**, *102*, 2663.
- (19) Galwey, A. K.; Brown, M. E. *Thermal Decomposition of Ionic Solids*; Elsevier: Amsterdam, 1999.
- (20) Johnson, N. L.; Leone, F. C. *Statistics and Experimental Design in Engineering and the Physical Sciences*; J. Wiley & Sons: New York, 1977; Vol. I.
- (21) Massart, D. L.; Vandeginste, B. G. M.; Buydens, L. M. C.; de Jong, S.; Lewi, P. J.; Smeyers-Verbeke, J. *Handbook of Chemometrics and Qualimetrics, Part A*; Elsevier: Amsterdam, 1997.
- (22) Hatakeyama, T.; Quinn, F. X. *Thermal Analysis: Fundamentals and Applications to Polymer Science*; Wiley: New York, 1994.
- (23) Oyumi, Y.; Brill, T. B. *Combust. Flame* **1985**, *62*, 225.
- (24) Ames, D. S.; Allman, J. C.; Lee, Y. T. In *Chemistry of Energetic Materials*; Olah, G. A., Squire, D. R., Eds.; Academic Press: San Diego, 1991; p 27.
- (25) Zheng, W.; Rogers, E.; Coburn, M.; Oxley, J.; Smith, J. *J. Mass Spectrom.* **1997**, *32*, 525.
- (26) Garland, N. L.; McElvany, S. W. *Chem. Phys. Lett.* **1998**, *297*, 147.
- (27) Zhang, Y.; Bauer, S. H. *J. Phys. Chem. A* **1998**, *102*, 5846.
- (28) Polizter, P.; Seminario, J. M. *Chem. Phys. Lett.* **1993**, *207*, 27.